An Evolutionary Method for Joint Optimization of UAV Path and Camera Direction Planning with Optional Viewpoints

Yifeng Sheng[1], Ning Xue[1*], Jiayi Dong[1], Libin Hong[2], Ruibin Bai[1], Heshan Du[1]

[1]School of Computer Science, University of Nottingham Ningbo China, Ningbo, China

[2]School of Information Science and Technology, Hangzhou Normal University, Hangzhou, China

***Abstract*—This paper addresses the Unmanned Aerial Vehicle (UAV) path planning problem with optional viewpoints, formulated as a joint optimization that considers surface coverage quality and flight energy consumption. The problem involves strong interdependence among viewpoint selection, path sequencing, and camera orientation, resulting in a large-scale combinatorial challenge that cannot be efficiently solved by off-the-shelf linear programming solvers. To tackle this, we develop a dual-layer chromosome genetic algorithm (GA) that encodes both UAV paths and camera directions. The GA employs adjacency-preserving edge-recombination crossover, feasibility-aware node replacement mutation, and a coverage repair operator, enabling constraint-preserving search while satisfying the sample point coverage requirement. Experiments on urban 3D scenes confirm that the GA consistently produces feasible solutions, achieving near-optimal quality on the majority of instances and solving large-scale problems intractable for Gurobi with a 94% time reduction, thereby demonstrating superior scalability and efficiency for UAV photogrammetric planning.**

***Index Terms*—genetic algorithm, hybrid encoding, UAV path planning, 3D reconstruction**

I. Introduction

UAV–based photogrammetry has been widely adopted in large-scale surveying and mapping tasks due to its high flexibility, efficiency, and relatively low operational cost [1]. In practical UAV mapping missions, planning strategies must simultaneously maximize scene coverage while minimizing energy consumption and the number of captured images, all of which are critical to ensuring data completeness, mission feasibility, and processing efficiency. These three objectives are inherently conflicting, making UAV photogrammetric planning a typical multi-objective optimization problem.

The planning process involves two strongly coupled components: UAV flight path planning and camera pose planning. The flight path determines the spatial sequence of UAV positions, whereas the camera pose directly affects the visibility and coverage quality of the target area. When these two components are jointly considered, the resulting problem can be formulated as a large-scale mixed-integer nonlinear programming (MINLP) problem [2], whose computational complexity increases rapidly with the number of candidate viewpoints and pose configurations. As a result, solving the integrated problem using exact optimization methods becomes computationally intractable for realistic scenarios.

To reduce computational complexity, most existing studies adopt a sequential strategy that first determines viewpoints and then computes a feasible path [3]. However, this decomposition ignores the strong coupling between path and camera decisions, often leading to suboptimal solutions.

In this paper, we propose a GA-based approach for integrated UAV photogrammetric planning. A dual-layer chromosome encoding scheme is developed to represent UAV paths and camera poses. To address the strong coupling and feasibility requirements, problem-specific genetic operators are designed to guide the evolutionary search. This design enables the GA to explore a more effective solution space than conventional sequential methods.

The proposed GA is validated against exact solutions from Gurobi [4]. It produces high-quality solutions within 10 minutes, with deviations under 10% for small instances, and remains feasible for large instances where Gurobi fails. This demonstrates its practical suitability for UAV photogrammetric planning.

The main contributions of this paper are summarized as follows:

- An integrated multi-objective formulation for UAV photogrammetric planning that jointly considers flight paths and camera poses.
- A dual-layer chromosome encoding scheme tailored to the coupled path–pose optimization problem.
- Customized genetic operators that ensure solution feasibility and enhance search efficiency.

The rest of the paper is organized as follows. Section II reviews related work. Section III formulates the UAV path planning problem as a multi-objective optimization with energy, coverage, and photo count objectives. Section IV presents the proposed dual-layer chromosome genetic algorithm, including encoding, crossover, mutation, and repair. Section V reports experiments and analyzes performance. Section VI concludes and discusses future work.

II. Related Work

UAVs have become a crucial platform for large-scale 3D reconstruction due to their ability to capture images from

*Corresponding author: Ning Xue (email: ning.xue@nottingham.edu.cn)

varied altitudes and otherwise inaccessible viewpoints [5]. High-quality reconstruction depends not only on the number of acquired images but also on optimal viewpoint selection and trajectory planning, as excessive data may introduce redundancy and computational overhead, while UAV battery limitations impose operational constraints [5]. Efficient algorithms for viewpoint and path planning are therefore essential, particularly for reconstructing complex structures. Existing methods for UAV-based reconstruction can be broadly categorized as model-based and model-free. Model-based strategies leverage coarse initial models to generate viewpoints and flight paths, often following an explore-then-exploit paradigm: preliminary exploration builds a geometric proxy, followed by optimized trajectory computation to maximize reconstruction quality. Early works often treated viewpoint selection and path planning independently. For example, He et al. [6] proposed a multi-UAV coordination framework using multi-objective particle swarm optimization for path planning but did not directly optimize 3D reconstruction quality. Hepp et al. [5] employed a building-scale reconstruction system with approximate camera models, enabling submodular optimization to estimate each candidate viewpoint's information gain, and recursively selected the most informative viewpoints [7].

A more common paradigm separates viewpoint selection and path planning into sequential stages. Hoppe et al. [8] applied greedy selection to maximize surface coverage and maintain sufficient overlap. Martin et al. [9] used a two-phase genetic algorithm: first optimizing viewpoint selection, then solving a TSP to minimize travel time. Jing et al. [10] formulated viewpoint selection as a modified Set Covering Problem with coverage and connectivity constraints. Other notable approaches include adaptive view planning [11], building-boundary-guided flights [12], hierarchical divide-and-conquer strategies [13], and sampling-based adaptive methods in urban environments [14], [15].

Only a few studies attempt joint optimization of viewpoint selection and trajectory planning. Roberts et al. [16] formulated the problem as an Orienteering Problem, determining camera orientations to maximize coverage and connecting viewpoints within a travel budget [17]. Koch et al. [18] proposed a semantic-aware explore-and-exploit strategy, sampling viewpoints around target objects and jointly optimizing reconstruction quality and path length. Zhang et al. [19] introduced a unified RRT*-based framework that simultaneously optimizes coverage, information efficiency, and trajectory smoothness.

Despite these advances, existing methods often focus on either sequential planning or heuristic joint optimization, leaving opportunities for more comprehensive approaches that integrate multi-objective criteria, environmental complexity, and operational constraints, which is the focus of this study.

III. Problem Description and Mathematical Formulation

Before formally defining the problem, we illustrate the UAV path planning scenario (Fig. 1). The 3D scene consists of surface sample points, while candidate viewpoints indicate

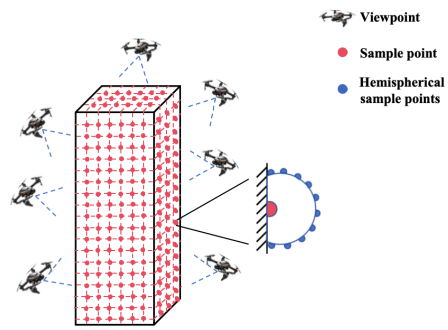

Fig. 1. UAV path planning scenario with sample points, candidate viewpoints, and hemispherical coverage.

potential UAV positions. Each viewpoint can capture images in a limited set of directions. Around each sample point, an upper hemisphere aligned with the surface normal is constructed, with discrete hemisphere points used to evaluate coverage: a point is covered if at least one UAV camera can observe it. The goal is to plan a UAV tour by selecting which viewpoints to visit, their camera directions, and the visiting order, so that coverage is maximized, energy consumption is minimized, and the number of photos is controlled.

A. Problem Definition

We consider an aerial coverage path planning problem for UAV-based photogrammetry, in which the UAV must visit a subset of candidate viewpoints while selecting appropriate camera directions to ensure sufficient coverage of a set of sampled surface points. The objective is to jointly optimize the flight tour, viewpoint visitation, and camera direction selection, such that the total energy consumption is minimized and the overall coverage quality is maximized. Let $\mathcal{V} = \{v_1, v_2, \ldots, v_n\}$ denote the set of candidate viewpoints, and let $\mathcal{T} \in \mathcal{V}$ be the subset of mandatory viewpoints that must be visited. The UAV departs from a predefined starting viewpoint $v_1 \in \mathcal{T}$. A tour is defined as a closed path visiting a selected subset of viewpoints while satisfying standard degree and connectivity constraints. Let $\mathcal{W} = \{w_1, w_2, \ldots, w_m\}$ be the set of sampled surface points requiring coverage. For each viewpoint, the UAV may select one camera direction from a finite set of uniformly distributed direction vectors $\mathcal{A}$. A camera pose is thus defined as a viewpoint–direction pair (v_k, a). This problem integrates tour optimization, coverage assurance, and direction assignment. For clarity, the main notations used throughout the paper are summarized in Table I.

B. Energy Consumption Model

The total energy consumption for the UAV traveling from viewpoint v_i to v_j is computed as

$$\begin{aligned} e_{ij} = &P_{\text{prop}}(d_{ij}) \\ &+ P_{\text{climb}}(\max(\Delta h_{ij}, 0)) \\ &+ P_{\text{descend}}(\max(-\Delta h_{ij}, 0)) \end{aligned} \tag{1}$$

TABLE I
MODEL NOTATIONS

Symbol	Description
Sets	
$\mathcal{V}$	Viewpoints set $\{v_1, \ldots, v_n\}$
$\mathcal{T}$	Mandatory viewpoints, v_1 is start
$\mathcal{W}$	Sampling points $\{w_1, \ldots, w_m\}$
$\mathcal{A}$	Discrete shooting directions
$\mathcal{E}$	Edge set between viewpoints
$\mathcal{S}_\ell$	Feasible viewpoint–direction pairs covering w_ℓ
$\mathcal{H}_\ell$	Discrete hemisphere points of w_ℓ
$\mathcal{D}_\ell$	Coverage indicator matrix of w_ℓ
Indices	
i, j, k	Viewpoint indices
ℓ	Sampling point index
a	Direction index
h	Hemisphere point index
Parameters	
e_{ij}	Energy cost between v_i and v_j
$d_{\ell h}^{ka}$	Coverage coefficient
γ_{lh}	Weight of hemisphere point (ℓ, h)
N_{lh}	Number of feasible (v_k, a) covering (ℓ, h)
Decision Variables	
x_{ij}	1 if edge (i, j) selected
y_k	1 if viewpoint v_k visited
z_{ka}	1 if photo taken at (v_k, a)
s_{lh}	1 if hemisphere point (ℓ, h) covered

where d_{ij} is the three-dimensional Euclidean distance between viewpoints, and Δh_{ij} is the altitude difference, with positive values for ascent and negative for descent. The functions P_{prop},P_{climb},$P_{descend}$ represent power consumption for horizontal flight, climbing, and descending, respectively.

C. Coverage Model

Following the approach of Roberts et al. [3], the coverage quality of each sampled surface point is approximated by the coverage area on its upper hemisphere.

1) Hemisphere Sampling and Coverage Indicator Matrix: For each sampled point $w_\ell \in \mathcal{W}$, an upper hemisphere centered at w_ℓ is constructed, with its axis aligned with the surface normal at that point. A finite set H_ℓ of $\mathcal{K}$ discrete points is uniformly sampled on this hemisphere to model visibility. For each camera pose (v_k, a) , we determine whether a hemispherical point $h \in H_\ell$ is visible from that pose based on geometric and visibility constraints. This relationship is encoded in a binary coverage indicator matrix $\mathcal{D}$, where

$$d_{\ell h}^{ka} = \begin{cases} 1, & \text{if point } h \text{ on the hemisphere of } w_\ell \\ & \text{is visible from } (v_k, a), \\ 0, & \text{otherwise.} \end{cases} \tag{2}$$

2) Coverage Indicator Variable: We define a binary coverage indicator variable $s_{\ell h}$ for each hemispherical point $h \in \mathcal{H}_\ell$. This variable is defined as

$$s_{\ell h} = \begin{cases} 1, & \text{if } \sum_{a \in \mathcal{A}} d_{\ell h}^{ka} \, z_{ka} \geq 1, \ \exists v_k \in \mathcal{V}, \\ 0, & \text{otherwise.} \end{cases} \tag{3}$$

That is, $s_{\ell h}$ equals 1 if at least one selected viewpoint–direction pair covers the hemispherical point (ℓ, h). To strengthen the formulation, we introduce the parameter

$$\mathcal{N}_{\ell h} = \left\{ (v_k, a) \in \mathcal{S}_\ell \ : \ d_{\ell h}^{ka} = 1 \right\} \tag{4}$$

which represents the total number of viewpoint–direction pairs that can potentially cover point (ℓ, h). This parameter is precomputed and used in the forcing constraint to tightly link the binary variable $s_{\ell h}$ with the underlying coverage condition.

3) Coverage Weighting: Since different regions on the hemispherical surface contribute unequally to the overall coverage quality, a weighting factor γ_h is assigned to each hemispherical point. The weight is defined as

$$\gamma_h = \cos \theta_h \tag{5}$$

where θ_h denotes the angle between the vector corresponding to point h on the hemisphere and the surface normal of the sampled point w_ℓ. This weighting scheme emphasizes coverage near the normal direction, which is typically more critical for photogrammetric reconstruction quality. The total coverage reward is then computed as the weighted sum of all covered hemispherical points across all sampled surface points.

D. Integrated Problem Formulation

In this paper, we merge the three normalized objectives into a single minimization function. This scalarization approach is motivated by two key factors. First, it provides users with the necessary flexibility to prioritize between UAV energy consumption and coverage quality for 3D reconstruction by tuning the objective weights. Second, formulating a single-objective problem allows us to rigorously benchmark the performance of our designed heuristic against a lower bound obtained from a standard linear programming solver. Specifically, the objective function consists of three sub-objectives: UAV energy consumption, coverage, and photo count. Each sub-objective is first normalized by its respective maximum value:

$$\tilde{f}_{\text{energy}} = \frac{\sum_{i \neq j} e_{ij} x_{ij}}{\max\left(\sum e_{ij} x_{ij}\right)}, \tag{6}$$

$$\tilde{f}_{\text{coverage}} = \frac{\sum_{w_l \in W} \sum_{h \in H_l} \gamma_{lh} s_{lh}}{\max\left(\sum \gamma_{lh} s_{lh}\right)}, \tag{7}$$

$$\tilde{f}_{\text{photo}} = \frac{\sum z_{ka}}{\max\left(\sum z_{ka}\right)} \tag{8}$$

The normalized objectives are then combined into a single minimization function:

$$\text{Minimize } \tilde{f}_{\text{energy}} + (1 - \tilde{f}_{\text{coverage}}) + \tilde{f}_{\text{photo}} \tag{9}$$

Constraints include:

- Path structure and camera orientation assignment constraints ensure that each selected viewpoint is assigned at least one feasible camera shooting direction. At the same time, by restricting the in-degree and out-degree of each activated node, path continuity is enforced, and disconnected subtours are eliminated, so that all selected viewpoints form a single connected UAV flight path.
- Coverage logic linking constraints are introduced to establish the relationship between the hemisphere coverage variable s_{lh} and the viewpoint–orientation decisions. A

hemisphere point can be marked as covered only if at least one selected viewpoint with one of its shooting directions provides a visible observation of that hemisphere point, thereby ensuring that multi-view geometric coverage requirements are satisfied.

- Reconstruction accuracy constraint: each sampling point must be captured at least 3 times

$$\sum_{(v_k,a)\in S_\ell} z_{ka} \geq 3, \qquad \forall w_\ell \in W \tag{10}$$

The decision variables $x_{ij}, y_k, z_{ka}, s_{lh}$ are binary, representing edge selection, node visitation, direction selection, and coverage decisions, respectively.

IV. Genetic Algorithm Design

This study develops a customized GA for UAV path planning with optional viewpoints. Unlike conventional works in the literature that adopt (meta-)heuristics, as reviewed in Section II, the proposed algorithm simultaneously optimizes both the path sequence and the shooting directions for each viewpoint, resulting in chromosomes composed of a path layer and an orientation layer. The problem is particularly challenging because not all candidate viewpoints are required to be visited, each sample point must be covered multiple times (i.e., at least three), and the path must satisfy UAV adjacency and energy constraints. Standard GAs cannot directly ensure solution feasibility or coverage requirements. To address these challenges, the algorithm incorporates an adjacency-aware edge recombination crossover (ERX) [20] with Lin–Kernighan (LK) [21] local optimization to refine paths, a unified orientation fusion mechanism to generate offspring directions, a selective node replacement mutation to explore alternative viewpoint combinations, and a sample point coverage repair operator to enforce coverage constraints (see Algorithm 1 for the complete GA procedure). These mechanisms allow the algorithm to jointly optimize viewpoint selection and path topology while maintaining path continuity and adjacency feasibility.

A. Encoding

The chromosome employs a two-layer encoding to jointly optimize UAV path planning and camera direction selection (see Fig. 2). The first layer encodes the flight tour: each gene corresponds to a candidate viewpoint, and the gene value indicates its next viewpoint in the path. The second layer encodes camera orientations: each gene corresponds to a viewpoint, and the gene value represents a selected camera direction from a finite set of discrete options. This design enables the simultaneous optimization of UAV routing and imaging configuration.

B. Crossover

In the crossover stage of the GA, the path layer uses ERX to inherit edges from the parents, followed by LK local optimization to refine the offspring paths while maintaining adjacency constraints. The ERX procedure constructs an adjacency table from both parents and iteratively selects the

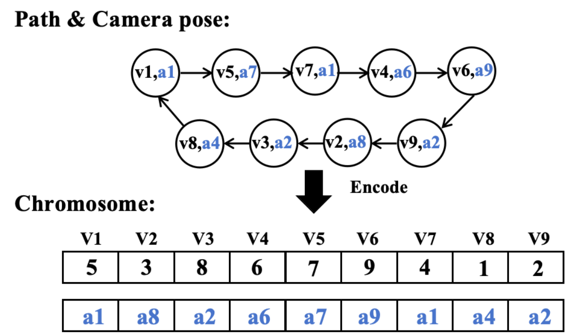

Fig. 2. Encoding

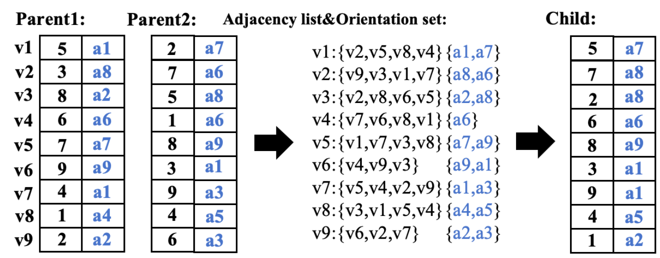

Fig. 3. Edge recombination crossover

next gene for the offspring based on adjacency information, prioritizing common edges and minimizing repeated visits until a complete path is generated (see Fig. 3 for an illustration of the ERX process). Parent pairs are produced using a two-stage selection strategy: individuals are ranked according to fitness, and selection probabilities are assigned based on ranking to construct a mating pool of the same size as the population through sampling with replacement; two distinct individuals are then uniformly randomly selected from the mating pool for crossover.

For the orientation layer, the candidate shooting directions from both parent solutions are first unified, after which a subset of feasible directions is selected to construct the offspring. The resulting orientation information is then re-encoded into the chromosome.

C. Mutation

In the mutation stage of the genetic algorithm, the path layer employs a selective node replacement operator, where a proportion p_{sel} of the selected viewpoints are randomly removed (parameter values are listed in Table II). For each removed node, an unvisited candidate viewpoint whose predecessor and successor can both be legally connected is selected to replace it, ensuring path continuity and adjacency constraint satisfaction. The replaced nodes are not reinserted into the path. This operator enables the simultaneous exploration of alternative viewpoint combinations and refinement of path topology while preserving the original path structure.

For the orientation layer, mutation is applied to a proportion p_{sel} of the selected viewpoints, where for each selected

Algorithm 1 Genetic Algorithm for UAV Path and Camera Direction Planning

Require: Population size N, maximum generations G
Ensure: Best chromosome (path + camera directions)
Initialize a feasible dual-layer population
for $g = 1$ to G **do**
  Evaluate fitness and construct mating pool
  for each parent pair **do**
    Crossover:
      Path layer: apply adjacency-aware ERX with LK refinement
      Direction layer: unify parent directions & select a feasible subset
    Mutation:
      Path layer: replace p_{sel} viewpoints with feasible unvisited nodes
      Direction layer: update p_{sel} viewpoints from candidates
    Repair:
      Enforce triple-coverage constraint
  end for
  Evaluate offspring and update population with elitism
end for
return Best chromosome

TABLE II
GENETIC ALGORITHM PARAMETERS

Parameter	Symbol	Value
Population size	N	100
Max generations	G	300
Crossover probability	p_c	0.6
Mutation rate	p_m	0.05
Mutation selection proportion	p_{sel}	0.02

viewpoint a subset of shooting directions is randomly chosen from its candidate directions, and the updated orientation information is re-encoded into the chromosome.

D. Repair

To ensure that each sample point is covered at least three times, a path repair operator is incorporated into the GA. This operator is applied after each crossover and mutation step to guarantee that newly generated offspring chromosomes satisfy the coverage constraints. The operator first counts the number of times each sample point is covered by the viewpoints along the chromosome path. For under-covered points, it first attempts to add additional shooting directions to existing path viewpoints to increase coverage. If coverage remains insufficient, unvisited candidate viewpoints capable of covering the sample point are selected, and feasible insertion positions are identified where both predecessor and successor satisfy adjacency constraints. The optimal insertion position is chosen based on minimum energy increment, and the new node along with its shooting directions is inserted into the path. This procedure preserves the original path structure while repairing coverage constraints and enabling local topological optimization.

V. Experimental Results and Analysis

A. Experimental Setup

Experiments were conducted on a desktop with an Intel Core i5 CPU and 32 GB RAM. The proposed GA was implemented in Python (v3.9.13), with Gurobi Optimizer (v12.0.3) used as an exact solver for comparison. The key GA parameters (see Table II) were determined via a Taguchi L9 (see Table III) experiment to ensure robust performance.

TABLE III
TAGUCHI L9 EXPERIMENT RESULTS FOR GA PARAMETERS

Run	Population	Crossover rate	Mutation rate	Fitness
1	20	0.6	0.05	0.983219
2	20	0.8	0.10	0.984340
3	20	0.9	0.20	0.994819
4	50	0.8	0.05	0.973298
5	50	0.9	0.10	0.981305
6	50	0.6	0.20	0.973470
7	100	0.9	0.05	0.952963
8	100	0.6	0.10	0.969864
9	100	0.8	0.20	0.988792

B. Dataset and Preprocessing

The building mesh data used in this study are derived from the Hong Kong Common Spatial Data Infrastructure [22], the UAV Pathplanning dataset [23], and the UrbanScene3D dataset [24]. The raw data were processed and categorized into small (where the number of candidate viewpoints is less than 180) and large instances. Each instance contains sample points, viewpoints, and associated attributes, as well as adjacency information for the candidate viewpoints and coverage information for the camera poses. The sample points and initial viewpoint set were selected and supplemented to ensure that each sample point is covered by multiple view frustums, producing a complete viewpoint set that satisfies multi-view coverage requirements.

C. Results and Analysis

Table IV compares normalized fitness values and computation times between the proposed GA and Gurobi. On small-scale instances ($<$ 180 viewpoints), the GA achieves solutions close to those of Gurobi, with fitness gaps within 2–16% (9% on average) while reducing computation time by over 94% (completing in under 10 minutes compared to over 3 hours for Gurobi). On large-scale instances ($>$ 180 viewpoints) where Gurobi fails to return a feasible solution within 8 hours, the GA reliably generates feasible solutions within approximately 20–40 minutes. The standard deviation across 20 independent runs remains low ($\pm$ 0.0022–0.0101 for small instances, $\pm$ 0.0042–0.0069 for large instances), confirming the stability and repeatability of the algorithm.

Overall, these results demonstrate that the proposed GA delivers practical near-optimal performance on tractable instances while scaling effectively to larger problems that are beyond the reach of exact solvers, offering a favorable trade-off between solution quality and computational efficiency.

VI. Conclusion And Future Work

This paper presents a tailored GA for UAV path planning with optional viewpoints, integrating adjacency-aware ERX crossover, selective mutation, and a coverage repair operator to ensure feasibility. Experiments on urban 3D scenes of different

TABLE IV
PERFORMANCE COMPARISON BETWEEN GUROBI AND GA

Instance	Gurobi (Fitness / Time, s)	GA Fitness	GA Time (s)
Small instances (< 180)			
building1	0.9472 / 18792	0.9660 ± 0.0049	378.0 ± 20.2
building2	0.8847 / 10958	0.9642 ± 0.0101	399.0 ± 14.0
building3	0.8992 / 18295	1.0115 ± 0.0089	275.0 ± 8.9
building4	0.9067 / 16704	1.0555 ± 0.0039	334.7 ± 23.0
building5	0.9602 / 14544	1.0034 ± 0.0022	355.0 ± 19.0
Large instances (> 180)			
NY-1	N/A / > 28800	0.9781 ± 0.0042	1274.7 ± 108.7
GOTH-1	N/A / > 28800	1.0040 ± 0.0046	2452.3 ± 183.5
Shenzhen_147	N/A / > 28800	1.0795 ± 0.0065	1644.0 ± 65.2
Suzhou_308	N/A / > 28800	1.1703 ± 0.0069	1745.7 ± 141.4

Note: N/A means the exact solution could not be obtained by Gurobi within the time limit. The GA results are reported as the mean $\pm$ standard deviation from 20 independent runs. All values are normalized fitness values combining energy, coverage, and photo count. For instances solved by Gurobi, the optimality gap is less than 1%.

scales show that the GA consistently generates paths satisfying multi-view coverage constraints with high solution quality.

The proposed algorithm effectively balances scalability with solution quality, solving large instances that are intractable for Gurobi while offering about a 20 times speedup and maintaining solution quality within 9% on most instances. This demonstrates its practical suitability for large-scale UAV photogrammetric planning.

Future work includes extending the approach to dynamic environments, considering moving obstacles and time-varying coverage requirements. Additionally, integrating multi-objective optimization techniques could further balance energy consumption, coverage precision, and flight time, making the method more applicable to real-world UAV operations. Furthermore, while this study employs Gurobi as the primary baseline for performance comparison, future work will incorporate additional heuristic and metaheuristic approaches, along with a broader range of benchmark datasets, to provide a more comprehensive evaluation of the proposed method.

ACKNOWLEDGMENT

This project was funded by both Ningbo Tianyi Design Research of Surveying and Mapping Co. Ltd. under Project TYCH-2025-001 (Research on Trajectory Optimization Technology for UAV Nap-of-the-Object Photogrammetry) and the Ningbo Science and Technology Bureau through the Ningbo Commonweal Programme (Project ID 2024S057). The authors also used an AI-based language editing tool to improve the clarity and readability of the manuscript.

REFERENCES

[1] F. Nex and F. Remondino, "Uav for 3d mapping applications: a review," *Applied geomatics*, vol. 6, no. 1, pp. 1–15, 2014.

[2] E. Galceran and M. Carreras, "A survey on coverage path planning for robotics," *Robotics and Autonomous systems*, vol. 61, no. 12, pp. 1258–1276, 2013.

[3] M. Roberts, D. Dey, A. Truong, S. Sinha, S. Shah, A. Kapoor, P. Hanrahan, and N. Joshi, "Submodular trajectory optimization for aerial 3d scanning," in *Proceedings of the IEEE International Conference on Computer Vision*, 2017, pp. 5324–5333.

[4] Gurobi Optimization, LLC, "Gurobi Optimizer Reference Manual," 2026. [Online]. Available: https://www.gurobi.com

[5] B. Hepp, "Planning for autonomous micro-aerial vehicles with applications to filming and 3d modeling," Ph.D. dissertation, ETH Zurich, 2018.

[6] W. He, X. Qi, and L. Liu, "A novel hybrid particle swarm optimization for multi-uav cooperate path planning," *Applied Intelligence*, vol. 51, no. 10, pp. 7350–7364, 2021.

[7] C. Chekuri and M. Pal, "A recursive greedy algorithm for walks in directed graphs," in *46th annual IEEE symposium on foundations of computer science (FOCS'05)*. IEEE, 2005, pp. 245–253.

[8] C. Hoppe, A. Wendel, S. Zollmann, K. Pirker, A. Irschara, H. Bischof, and S. Kluckner, "Photogrammetric camera network design for micro aerial vehicles," in *Computer vision winter workshop (CVWW)*, vol. 8, 2012, pp. 1–3.

[9] R. A. Martin, I. Rojas, K. Franke, and J. D. Hedengren, "Evolutionary view planning for optimized uav terrain modeling in a simulated environment," *Remote Sensing*, vol. 8, no. 1, p. 26, 2015.

[10] W. Jing, J. Polden, P. Y. Tao, W. Lin, and K. Shimada, "View planning for 3d shape reconstruction of buildings with unmanned aerial vehicles," in *2016 14th International Conference on Control, Automation, Robotics and Vision (ICARCV)*. IEEE, 2016, pp. 1–6.

[11] C. Peng and V. Isler, "Adaptive view planning for aerial 3d reconstruction," in *2019 International Conference on Robotics and Automation (ICRA)*. IEEE, 2019, pp. 2981–2987.

[12] O. Sharma, N. Arora, and H. Sagar, "Image acquisition for high quality architectural reconstruction." in *Graphics Interface*, 2019, pp. 18–1.

[13] C. Cao, J. Zhang, M. Travers, and H. Choset, "Hierarchical coverage path planning in complex 3d environments," in *2020 IEEE International Conference on Robotics and Automation (ICRA)*. IEEE, 2020, pp. 3206–3212.

[14] F. Yan, E. Xia, Z. Li, and Z. Zhou, "Sampling-based path planning for high-quality aerial 3d reconstruction of urban scenes," *Remote Sensing*, vol. 13, no. 5, p. 989, 2021.

[15] X. Liu, Z. Ji, H. Zhou, Z. Zhang, P. Tao, K. Xi, L. Chen, and J. Marcato Junior, "An object-oriented uav 3d path planning method applied in cultural heritage documentation," *ISPRS Annals of the Photogrammetry, Remote Sensing and Spatial Information Sciences*, vol. 1, pp. 33–40, 2022.

[16] M. Roberts, S. Shah, D. Dey, A. Truong, S. Sinha, A. Kapoor, P. Hanrahan, and N. Joshi, "Submodular trajectory optimization for aerial 3d scanning," in *2017 IEEE International Conference on Computer Vision (ICCV)*, 2017, pp. 5334–5343.

[17] A. Gunawan, H. C. Lau, and P. Vansteenwegen, "Orienteering problem: A survey of recent variants, solution approaches and applications," *European Journal of Operational Research*, vol. 255, no. 2, pp. 315–332, 2016.

[18] T. Koch, M. Körner, and F. Fraundorfer, "Automatic and semantically-aware 3d uav flight planning for image-based 3d reconstruction," *Remote Sensing*, vol. 11, no. 13, p. 1550, 2019.

[19] H. Zhang, Y. Yao, K. Xie, C.-W. Fu, H. Zhang, and H. Huang, "Continuous aerial path planning for 3d urban scene reconstruction." *ACM Trans. Graph.*, vol. 40, no. 6, pp. 225–1, 2021.

[20] L. D. Whitley, T. Starkweather, and D. Fuquay, "Scheduling problems and traveling salesmen: The genetic edge recombination operator," in *International Conference on Genetic Algorithms*, 1989. [Online]. Available: https://api.semanticscholar.org/CorpusID:12884640

[21] S. Lin and B. W. Kernighan, "An effective heuristic algorithm for the traveling-salesman problem," *Operations Research*, vol. 21, no. 2, pp. 498–516, 1973.

[22] Census and Statistics Department, The Government of the Hong Kong Special Administrative Region. (2022) Comprehensive social security assistance. Composite Social Data Infrastructure Portal. [Online]. Available: https://portal.csdi.gov.hk/csdi-webpage/

[23] N. Smith, N. Moehrle, M. Goesele, and W. Heidrich, "Aerial path planning for urban scene reconstruction: a continuous optimization method and benchmark," *ACM Trans. Graph.*, vol. 37, no. 6, Dec. 2018. [Online]. Available: https://doi.org/10.1145/3272127.3275010

[24] L. Lin, Y. Liu, Y. Hu, X. Yan, K. Xie, and H. Huang, "Capturing, reconstructing, and simulating: the urbanscene3d dataset," in *European Conference on Computer Vision*. Springer, 2022, pp. 93–109.